DFT calculations of magnetic parameters for molybdenum complexes and hydroxymethyl intermediates trapped on silica surface

ARTICLE *in* SPECTROCHIMICA ACTA PART A MOLECULAR AND BIOMOLECULAR SPECTROSCOPY · APRIL 2006

Impact Factor: 2.35 · DOI: 10.1016/j.saa.2005.10.029 · Source: PubMed

2 AUTHORS:

Zbigniew Sojka
Jagiellonian University
207 PUBLICATIONS **2,117** CITATIONS

SEE PROFILE

Piotr Pietrzyk
Jagiellonian University
45 PUBLICATIONS **513** CITATIONS

SEE PROFILE

Available online at www.sciencedirect.com
SCIENCE DIRECT
Spectrochimica Acta Part A 63 (2006) 788–794
SPECTROCHIMICA ACTA PART A
www.elsevier.com/locate/saa

DFT calculations of magnetic parameters for molybdenum complexes and hydroxymethyl intermediates trapped on silica surface

Zbigniew Sojka [a,b,*], Piotr Pietrzyk [a]

[a] *Faculty of Chemistry, Jagiellonian University, ul. Ingardena 3, 30-060 Kraków, Poland*
[b] *Regional Laboratory of Physicochemical Analyses and Structural Research, ul. Ingardena 3, 30-060 Kraków, Poland*

Received 1 July 2005; received in revised form 23 September 2005; accepted 1 October 2005

Abstract

Density functional theory (DFT) calculations of EPR parameters and their structure sensitivity for selected surface paramagnetic species involved in oxidative dehydrogenation of methanol over silica grafted molybdenum catalyst were investigated. Two surface complexes, Mo_{4c}/SiO_2 and $\{O^- - Mo_{4c}\}/SiO_2$, as well as $^{\bullet}CH_2OH$ radical trapped on the SiO_2 matrix were taken as the examples. The spin-restricted zeroth order regular approximation (ZORA) implemented in the Amsterdam Density Functional suite was used to calculate the electronic ***g*** tensor for those species. The predicted values were in satisfactory agreement with experimental EPR results. Five different coordination modes of the $^{\bullet}CH_2OH$ radical on the silica surface were considered and the isotropic ^{13}C, ^{17}O, and ^{1}H hyperfine coupling constants (HFCC) of the resultant surface complexes were calculated. Structure sensitivity of the HFCC values was discussed in terms of the angular deformations caused by hydrogen bonding with the silica surface.

Keywords: EPR; DFT; ZORA; ***g*** Tensor; CH_2OH; HFCC; Molybdenum; Silica; Catalyst

1. Introduction

Radical intermediates are very reactive open-shell transients often involved in many important catalytic processes [1]. In the course of a surface reaction radicals are rapidly transformed into more stable species following various mechanisms such as surface electron transfer, recombination and disproportionation or more involved chain reactions. A particular feature of those processes is that they often involve migration of radicals on the surface.

Depending on the extent of the interactions with the surface, the adsorbed radicals can be considered as bound or itinerant species. The bound radicals are attached to the particular surface sites by forming chemical bonds, via electrostatic interactions or through hydrogen bonding. Such entities are usually sufficiently stable for their direct observation and structural characterization [2]. The interactions with the surface, however, give rise to considerable modifications of the geometry and electronic structure which may be reflected in their spectroscopic properties.

Electron magnetic resonance is the most powerful spectroscopic technique for characterization of the open-shell species entrapped on surfaces of various catalytic materials [2]. High sensitivity and specificity make it well-suited to investigate and characterize low abundant paramagnetic species, and to follow their fate during chemical transformations. However, heterogeneity of the investigated systems, speciation of paramagnetic centers and their frequent low symmetry may severely complicate the character of the resultant EPR spectra [3]. Analysis of such spectra and a molecular interpretation of the spin–Hamiltonian parameters is, thus, hardly possible without help of the advanced computer simulations supported by complementary quantum chemical calculations (computational spectroscopy).

Modern accurate ab initio approaches for calculation of ***g*** tensor components based on the multi-reference configuration interaction (MRCI) [4] and multi-configuration self-consistent-field (MCSCF) [5] methodologies are largely restricted to radicals or systems composed of light elements. Inclusion of all perturbation operators relevant for the electronic ***g*** tensor at the Breit–Pauli treating of the spin–orbit coupling is usually computationally too expensive. For larger systems, density functional theory (DFT), owing to the recent developments in the

* Corresponding author. Tel.: +48 12 663 22 24; fax: +48 12 634 05 15.
E-mail address: sojka@chemia.uj.edu.pl (Z. Sojka).

1386-1425/$ – see front matter © 2005 Elsevier B.V. All rights reserved.
doi:10.1016/j.saa.2005.10.029

relativistic theory of the $\boldsymbol{g}$ tensor, provides an attractive alternative [6,7]. There are several DFT implementations of the $\boldsymbol{g}$ tensor calculations reported in the literature, which basically fall into two major classes. Two-component approaches like zeroth-order regular approximation (ZORA) [8] include spin–orbit coupling treated variationally with the $\boldsymbol{g}$ tensor calculated as a first-order property. In one-component methods based on scalar relativistic approximation within the Pauli Hamiltonian [9], both the magnetic field and the spin–orbit coupling are treated as perturbations, leading to a second-order $\boldsymbol{g}$ tensor expression [10].

The theoretical methods of calculating the hyperfine coupling constants (HFCC) have mostly focused on organic radicals or systems composed of p-elements [11,12]. The more demanding transition-metal ion (TMI) containing systems are far more difficult, mainly due to the need of an accurate inclusion of the electron exchange and correlation along with the large basis sets required to correctly account for the spin polarization effects [13,14].

Most of the theoretical studies on the hyperfine structure have referred so far to radicals in vacuum [15]. There are, however, few cases where the interaction with surroundings was taken into account explicitly [16]. Structural and electronic modifications of trapped radicals brought about by the surface are manifested, i.e., in the change of their magnetic parameters. The aim of this paper is to calculate by means of the relativistic DFT methods the $\boldsymbol{g}$ and the hyperfine tensors of surface paramagnetic species involved in oxidative dehydrogenation of methanol over silica grafted molybdenum catalyst, such as Mo_{4c}/SiO_2, $\{O^-–Mo_{4c}\}/SiO_2$ and $^\bullet CH_2OH$ radical, and to explore the structure sensitivity of the magnetic parameters of the latter one.

2. Computational details

Using the normalized spin density, $\langle S_z\rangle^{-1}\Sigma_{\mu,\nu}P_{\mu\nu}^{\alpha-\beta}$, the principal interactions between the unpaired electron and the magnetic nuclei, the isotropic Fermi contact interaction a_{iso}^n and the anisotropic dipolar interaction T_{ij}^n, can be expressed to the first-order with the following equations [17]:

$$a_{iso}^n = \frac{4\pi}{3}\beta_e\beta_n g_e g_n \langle S_z\rangle^{-1}\sum_{\mu,\nu}P_{\mu\nu}^{\alpha-\beta}\langle\varphi_\mu(r_{kn})|\delta(r_{kn})|\varphi_\nu(r_{kn})\rangle \quad (1)$$

$$T_{ij}^n = \frac{1}{2}g_e\beta_e g_n\beta_n\langle S_z\rangle^{-1}\sum_{\mu,\nu}P_{\mu\nu}^{\alpha-\beta}\langle\varphi_\mu(r_{kn})|r_{kn}^{-5}(r_{kn}^2\delta_{ij} - 3r_{kn,i}r_{kn,j})|\varphi_\nu(r_{kn})\rangle \quad (2)$$

The isotropic component is, thus, directly proportional to the spin density $\rho^{\alpha-\beta}(r_n)\equiv\rho^\alpha(r_n)-\rho^\beta(r_n)$ at the corresponding nucleus n, whereas the anisotropic part T^n of the hyperfine tensor reflects the asymmetry of the spin density around each nucleus of interest. In the two-component ZORA, available in ADF package and used in this work, assuming that a Kramers doublet (Φ_1, Φ_2) describes the magnetic properties of the investigated paramagnet, the $\boldsymbol{g}$ tensor components are defined by the matrix elements $\Phi_{ij}^k = \langle\Phi_i|\partial H^Z/\partial B_k|\Phi_j\rangle$ in the following way [8]:

$$\begin{aligned} g_{kx} &= 4cRe\Phi_{12}^k = 4cRe\Phi_{21}^k \\ g_{ky} &= -4cIm\Phi_{12}^k = 4cIm\Phi_{21}^k \\ g_{kz} &= 4cRe\Phi_{11}^k = 4cRe\Phi_{22}^k \end{aligned} \quad (3)$$

where H^Z is the Zeeman Hamiltonian. From the g_{kl} values a G matrix can be produced, $G_{kl}=\sum_{i=1}^3 g_{ki}g_{li}$, which after diagonalization yields the principal values of $g_{kk}=\sqrt{G_{kk}}$.

Several different modes of attachment of the $^\bullet CH_2OH$ radical to the cluster that were considered include coordination via H-bonding either through hydroxyl and methyl hydrogen atoms or via oxygen and carbon lone pairs. Geometry optimization of the hydroxymethyl radical and its silica surface-trapped form was carried out by means of Gaussian03 program [18] with no symmetry restrictions at the spin-unrestricted level. As the exchange-correlation potential we used standard B3LYP [19,20] method with the all-electron 6-311G(d) basis set. The structures of the molybdenum surface complexes was obtained in a separate study using DMol [21] software developed by Accelrys Inc. [22] with the Becke [23], Perdew and Wang [24] potential. The double numerical basis set supplemented by polarization functions (DNP) was used. Silica surface was mimicked with finite clusters cut off from amorphous silica structure [25]. Two various clusters: **T2** corresponding to $\{Si_2O_3(OH)_4\}^{2-}$ and **T5** corresponding to $\{Si_5O_5(OH)_3H_7\}$, introduced in our earlier studies [26,27], were used to model the silica surface sites. The molybdenum complexes Mo_{4c}/SiO_2 and $\{O^-–Mo_{4c}\}/SiO_2$ were modeled with $\{Mo{=}O(OH)\}$/**T2** and $\{O–Mo{=}O(OH)\}$/**T2** clusters, respectively.

The hyperfine couplings for the optimized structures of the $^\bullet CH_2OH/SiO_2$ complexes were calculated with Gaussian03. The combination of the B3LYP exchange-correlation functional with the EPR-III, 6-311G(df) and LanL2DZ basis sets, justified in our earlier study [27], was used for this purpose. The $\boldsymbol{g}$ tensor calculations were carried out with the ADF suite [28,29] using the ZORA approach and gauge-including atomic orbitals (GIAO) [8,30]. Since the $\boldsymbol{g}$ tensor for many transition-metal complexes were shown to be essentially independent of the choice of a density functional [9], we applied simple VWN LDA method [31]. An all-electron triple-ζ Slater-type basis set with polarization functions was used.

3. Results and discussion

3.1. Formation of $^\bullet CH_2OH$ radical

Hydroxymethyl radicals are important transients in the low temperature oxidative dehydrogenation of methanol over silica grafted molybdenum catalyst (MoO_x/SiO_2) [32]. The active sites for this reaction are tetra-coordinated surface complexes of mononuclear molybdenum (Mo_{4c}/SiO_2) exhibiting an EPR signal characterized by $g_\perp = 1.926$ and $g_{||} = 1.755$. An O^- intermediate bound to molybdenum center, $\{O^-–Mo_{4c}\}/SiO_2$ with $g_\perp = 2.020$ and $g_\parallel = 2.005$, which plays a key role in the C–H bond activation, can be produced by interaction of N_2O at 373 K

Table 1
Comparison of the experimental and theoretical spin–Hamiltonian parameters for the key species involved in the formation of the hydroxymethyl radical over MoO_x/SiO_2 catalyst

Structure		$g_\perp$	$g_\parallel$	g_{av}	a_{iso} (G)
Mo_{4c}^{5+}—**T2**	Exp.	1.926	1.755		
	Theory	1.916 ($g_1 = 1.931$, $g_2 = 1.902$)	1.745		
Mo_{5c}^{6+}—O^-—**T2**[a]	Exp.	2.020	2.005		
	Theory	2.018 ($g_1 = 2.024$, $g_2 = 2.012$)	2.002		
Mo_{5c}^{6+}—O^-—**T2**[b]	Exp.	2.020	2.005		
	Theory	2.005 ($g_1 = 2.007$, $g_2 = 2.002$)	2.027		
Free $^\bullet CH_2OH$	Exp.			2.0034[c]	
	Theory			2.0035 ($g_1 = 2.0055$, $g_2 = 2.0029$, $g_3 = 2.0021$)	
$^\bullet CH_2OH$—**T5**	Exp.			2.0034	54[d], −19.3[e]
	Theory			2.0039 ($g_1 = 2.0054$, $g_2 = 2.0043$, $g_3 = 2.0021$)	55[d], −14.5[e]

[a] Tetragonal pyramid.
[b] Trigonal bipyramid.
[c] Ref. [38].
[d] ^{13}C.
[e] ^1H (CH_2).

with Mo_{4c}/SiO_2 [33]. The multi-step mechanism of methanol dehydrogenation involves formation of the $^\bullet CH_2OH$ radicals via hydrogen abstraction by O^- species bound to Mo, migration of hydroxymethyl radicals on the surface, and electroprotic conversion of $^\bullet CH_2OH$ to CH_2O accompanied by reduction of molybdenum. At temperatures below 140 K, the hydroxymethyl intermediates can be stabilized on the surface of silica. The Mo_{4c}/SiO_2 and $\{O^-—Mo_{4c}\}/SiO_2$ active centers, as well as the hydroxymethyl intermediates trapped on the silica matrix were previously characterized by EPR spectroscopy [32,33,34] and their parameters obtained from computer simulation are summarized in Table 1.

3.2. Structure of active sites and intermediates

The optimized geometry of the Mo_{4c}/**T2** surface complex epitomizing the Mo_{4c}/SiO_2 active centers of the silica grafted molybdenum catalyst is shown in Fig. 1a. The bidentate coordination of the molybdenyl ion to the silica framework exhibited a pseudo-tetrahedral structure with nearly equal Mo–O(Si) bond lengths ($\langle d_{Mo–O(Si)}\rangle = 1.954(3)$ Å), and the terminal Mo=O bond being much shorter ($d_{Mo=O} = 1.718$ Å). The O(Si)–Mo–O(Si) angle was equal to 98°, whereas, O=Mo–O(H) angle was slightly larger (117°). Although the local symmetry of molybdenum in such a surface complex is close to C_s, with the mirror plane passing through the Mo=O and Mo–O(H) bonds and bisecting the angle $\phi_{O(Si)–Mo–O(Si)}$, the symmetry of the $\boldsymbol{g}$ tensor is mainly determined by strong axial filed imposed by the molybdenyl bond. The singly occupied molecular orbital (SOMO) is mainly composed of the molybdenum $4d_{xy}$ orbital (Fig. 1b), giving rise to the experimentally observed pattern $g_\perp > g_\parallel$.

Structural modifications induced by incorporation of the O^- species into the coordination sphere of molybdenum to form the $\{Mo_{4c}—O^-\}$/**T2** surface complex are shown in Fig. 1c and d. Two possible coordination environments of Mo center include a square pyramid and a trigonal bipyramid geometry, with the O^- ligand in the equatorial position. Lengthening of the Mo=O bond and shortening of the equatorial bonds, in comparison to the parent tetra-coordinated complex were much more pronounced in the case of the trigonal bipyramid conformation ($d_{Mo=O} = 1.740$ Å, $\langle d_{Mo–O(Si)}\rangle = 1.933(2)$ Å) than for the square pyramid one ($d_{Mo=O} = 1.729$ Å, $\langle d_{Mo–O(Si)}\rangle = 1.922(4)$ Å).

The $^\bullet CH_2OH$ radical in gas phase exhibits two kinds of hydrogen atoms in the methyl group located in *cis* and *trans* positions with respect to hydroxyl group. The calculated distances from carbon to *cis* and *trans* hydrogen were equal to $d_{C–H\,cis} = 1.087$ Å and $d_{C–H\,trans} = 1.083$ Å, respectively, and the carbon–oxygen bond length was equal to $d_{C–O} = 1.374$ Å. The H_{trans}–C–H_{cis} angle $\delta_{H–C–H} = 120.9°$, whereas the dihedral angle $dih_{H–C–O–H}$ (defined by the intersection of the H–O–C and O–C–H_{cis} planes) was equal to −25.4°, indicating a distinct departure of the hydroxyl group from the methylene plane (H_{trans}–C–H_{cis}).

To investigate the influence of silica surface on the structure and magnetic properties of the trapped hydroxymethyl, the radical was attached to the **T5** cluster in five different coordination modes (Fig. 2). They epitomize interaction of the radical with the surface through hydrogen bonds either via the OH group (**I**), the CH_2 group (**II**), or by the OH and CH_2 groups simultaneously (**III**) or through the lone pairs of carbon (**IV**) and oxygen (**V**) atoms. The structures of the resultant van der Waals complexes are shown in Fig. 2. The strongest links with the surface are established when the radical is attached via the hydroxyl group either through the hydrogen bonding (structure **I**) or through the lone pair of oxygen (**V**), as it can be inferred from the shortest bond length (1.50–1.83 Å). The lengths of the hydrogen bonds made through the CH_2 group are distinctly longer (2.15–2.36 Å). Because of the energy difference of only few kcal/mol ($\Delta E = 4.7$ kcal/mol), as in the case of the coordination modes **II** and **III**, the energetic arguments alone may not be sufficient to determine the correct ground state geometry, so the resultant magnetic parameters may serve as the additional diagnostic features.

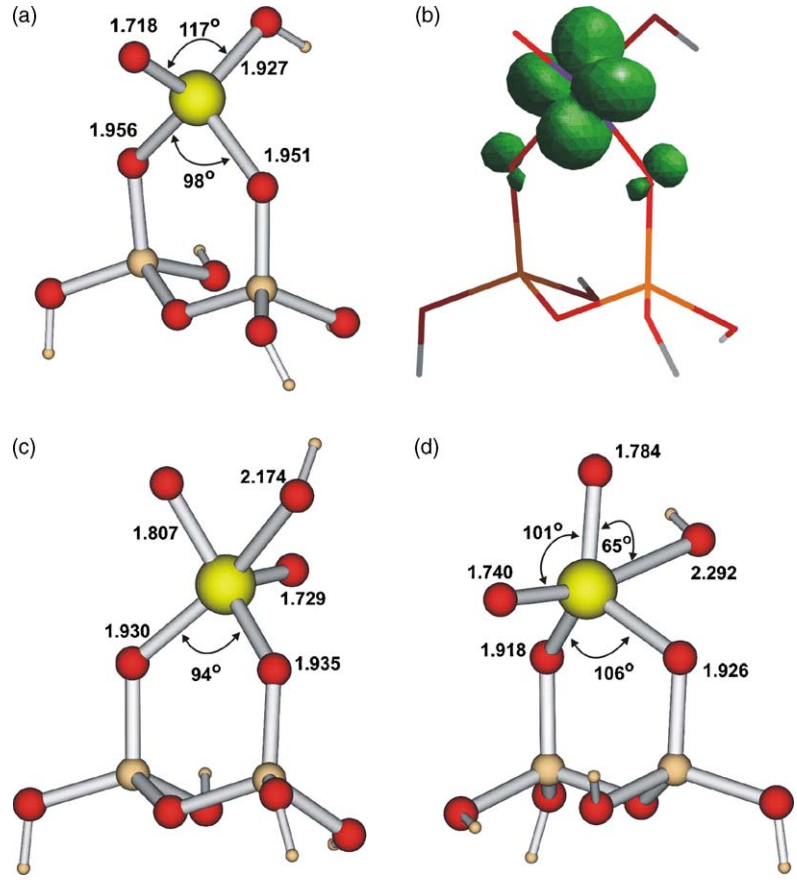

Fig. 1. Optimized structures of the {Mo═O(OH)}/**T2** cluster (a) along with the associated spin density distribution contour (b), and of the {O─Mo═O(OH)}/**T2** cluster in square pyramidal (c) and trigonal bipyramidal (d) conformations. Selected geometrical parameters are given in Å and degree.

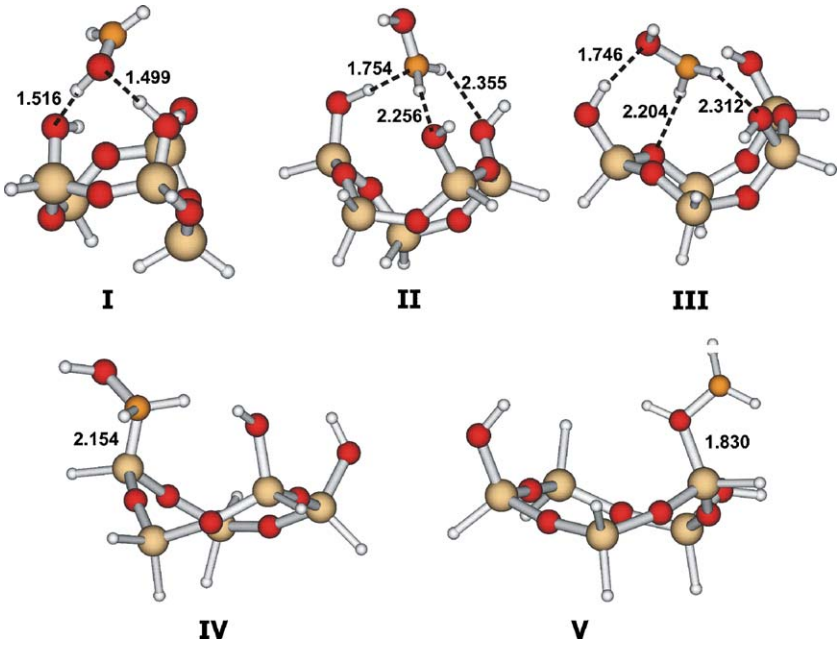

Fig. 2. Optimized structures of the hydroxymethyl radical trapped on the silica surface (**T5** cluster) for various coordination modes. Dashed lines indicate hydrogen bonds with their lengths given in Å.

3.3. Magnetic parameters

The calculated magnetic parameters of all investigated species are summarized in Table 1, together with the corresponding experimental values. From inspection of this table, we can readily infer that the ZORA/VWN approach was able to reproduce the $\boldsymbol{g}$ tensor components of the Mo_{4c}/SiO_2 and the $\{O^{-}{-}Mo_{4c}\}/SiO_2$ surface complexes quite satisfactorily. Two distinct values of $g_1 = 1.931$ and $g_2 = 1.902$ obtained for $Mo_{4c}{}^{5+}/SiO_2$ sites can be combined yielding $g_\perp = 1/2(g_1 + g_2) = 1.916$, to be compared with the experimental $g_\perp = 1.926$. A pronounced shift of the parallel component $g_\parallel = 1.745$ was well reproduced (the experimental value is equal to 1.755). Generally, the calculated values were systematically slightly too small comparing to experiment. Similar effect observed previously for d^1 systems has been assigned to the overestimation of the covalent character of the bonds formed by metal d orbitals by DFT method [35].

Even better agreement was achieved in the case of the ligand centered $\{O^{-}{-}Mo_{4c}\}/SiO_2$ radical complex. The calculated values with $g_\perp = 1/2(g_1 + g_2) = 2.018 > g_\parallel = 2.002$, obtained for the square pyramid structure, remain in a good agreement with the experimental values ($g_\perp = 2.020 > g_\parallel = 2.005$), in contrast to the trigonal bipyramid conformation, where a reversed order ($g_\parallel > g_\perp$) with respect to the experiment was observed ($g_\perp = 1/2(g_1 + g_2) = 2.005$ and $g_\parallel = 2.027$).

Magnetic properties of the $^{\bullet}CH_2OH$ radical are essentially determined by a large positive spin density on the carbon atom ($\rho_C = 0.95$), smaller one on the oxygen ($\rho_O = 0.11$), and tiny negative spin densities on the methyl ($\rho_{H(C)} = -0.03$) and hydroxyl ($\rho_{H(O)} = -0.004$) hydrogen atoms, induced by polarization of the C–H and O–H bonds, respectively. The HFCC values calculated at the B3LYP/EPR-III level were equal to $a_{iso}(^{13}C) = 44.9$ G, $a_{iso}(^{1}H_{cis}) = -15.12$ and $a_{iso}(^{1}H_{trans}) = -17.65$ G, nicely comparing with the experimental $|a_{iso}|$ values of 45.33, 17.65 and 18.53 G, respectively [36,37]. Such a good agreement confirms the adequacy of the adopted B3LYP/EPR-III scheme for HFCC calculation of radicals composed of light elements, in accordance with the previous literature data [11,16,38].

In the case of surface-trapped hydroxymethyl radicals the resolution of the conventional X-band EPR was too small to resolve the difference in the hyperfine splitting of both methyl protons, and the anisotropy of the $\boldsymbol{g}$ tensor as well. However, the average value of $\boldsymbol{g}$ factor ($g_{av} = 2.0034$), that could easily be determined from the experimental spectrum, is very close to that calculated with ZORA/VWN approach ($g_{av} = 1/3(g_1 + g_2 + g_3) = 2.0039$ for structure **I**. A good accordance was also observed in the case of $a_{iso}(^{13}C) = 55$ G and $a_{iso}(^{1}H) = -14.5$ G HFCC. These values are distinctly different form the corresponding values of the gas phase radical showing that upon trapping its molecular structure was considerably modified.

3.4. Structure sensitivity of HFCC for $^{\bullet}CH_2OH$ radical

Because of its dual nature involving spin delocalization and spin polarization, the isotropic coupling parameters are very sensitive toward changes in the geometry. For analysis of the structure sensitivity of HFCC for hydroxymethyl radical we have chosen a dihedral ($dih_{H–C–O–H}$) distortion angle to describe the rotation of the OH group around the C–O bond and a bending angle ($\delta_{H–C–H}$) to measure the deformation of the CH_2 group caused by the interaction with the environments (the SiO_2 surface). The flexibility of the $^{\bullet}CH_2OH$ radical was unraveled by calculating potential energy surface, which shows a flat shape in the vicinity of the minimum. Thus, the structure of this radical may easily be deformed even by the mere supramolecular interactions with the matrix like those due to hydrogen bonding.

At first, we tested the response of a_{iso} to angular distortion of the free hydroxymethyl radical. The results obtained for $a_{iso}(^{13}C)$ as a function of the bending $\delta_{H–C–H}$ and dihedral $dih_{H–C–O–H}$ angles are shown in the form of a 3D plot in Fig. 3. It is clear that ^{13}C hyperfine coupling is very sensitive to the bending deformation, whereas the sensitivity to the rotational distortion is less pronounced. Two clear local minima can be distinguished in the plot. The first one at $dih_{H–C–O–H} = -95^\circ$ corresponds to a nearly C_s symmetry of the $^{\bullet}CH_2OH$ radical, with the mirror plane defined by the C–O–H atoms. In such a case, the in-plane orbitals of the OH unit are directly admixed to the SOMO, giving rise to an increase of the $a_{iso}(^{1}H(O))$ value up to 41.2 G, at the expense of the carbon 2s contribution. A deeper minimum at $dih_{H–C–O–H} = 0^\circ$ was associated with a slightly nonplanar structure (the sum of angles around the C atom equals to 350°). For perfectly planar CH_2–O group a negative value of $a_{iso}(^{13}C)$ is expected, whereas non-planarity allows for carbon 2s admixture to the SOMO giving rise to the positive HFCC values. Since bending is the smallest for $dih_{H–C–O–H} = 0^\circ$, this contribution is reduced and consequently the $a_{iso}(^{13}C)$ exhibits its lowest value. The changes induced by the variation of the $\delta_{H–C–H}$ angle are more uniform. They can easily be accounted for by rehybridization of the carbon atom. Decrease of the H–C–H angle results in piramidization of the carbon and reduced involvement of the carbon 2s orbital in the SOMO. An analogous 3D plot for $a_{iso}(^{17}O)$ shows that the HFCC changes significantly only in the case of a very high deformation of the hydroxymethyl radical, being more sensitive to changes in the $\delta_{H–C–H}$ angle rather than to the $dih_{H–C–O–H}$ one. The maximum in the $a_{iso}(^{17}O)$ plot for $dih_{H–C–O–H} = -95^\circ$ is associated with a hyperconjugative transfer of the spin density from the carbon to the oxygen. The structure sensitivity of both methyl protons shows clearly different sensitivity to the $dih_{H–C–O–H}$ angle, whereas the influence to changes in the $\delta_{H–C–H}$ are more important and similar in magnitude. Resulting form the polarization of the C–H bond, the methylene protons' hyperfine coupling values essentially reflect the variation of the spin density at the carbon atom with $\delta_{H–C–H}$ that, in turn, is gauged by the $a_{iso}(^{13}C)$ value. As the $a_{iso}(^{1}H_{trans})$ is distinctly more affected than the $a_{iso}(^{1}H_{cis})$ coupling by the changes of the $dih_{H–C–O–H}$, such a deformation will increase the non-equivalence of the both protons. Thus, it can be taken as a sensitive diagnostic probe of the torsional deformation.

Noting the flexibility of the $^{\bullet}CH_2OH$ radical the isotropic hyperfine constants for ^{13}C, ^{17}O and ^{1}H nuclei were next calculated for five different silica-trapped van der Waals complexes shown in Fig. 2 to evaluate the influence of the steric effects on HFCC. The resultant HFCC and the actual values of the

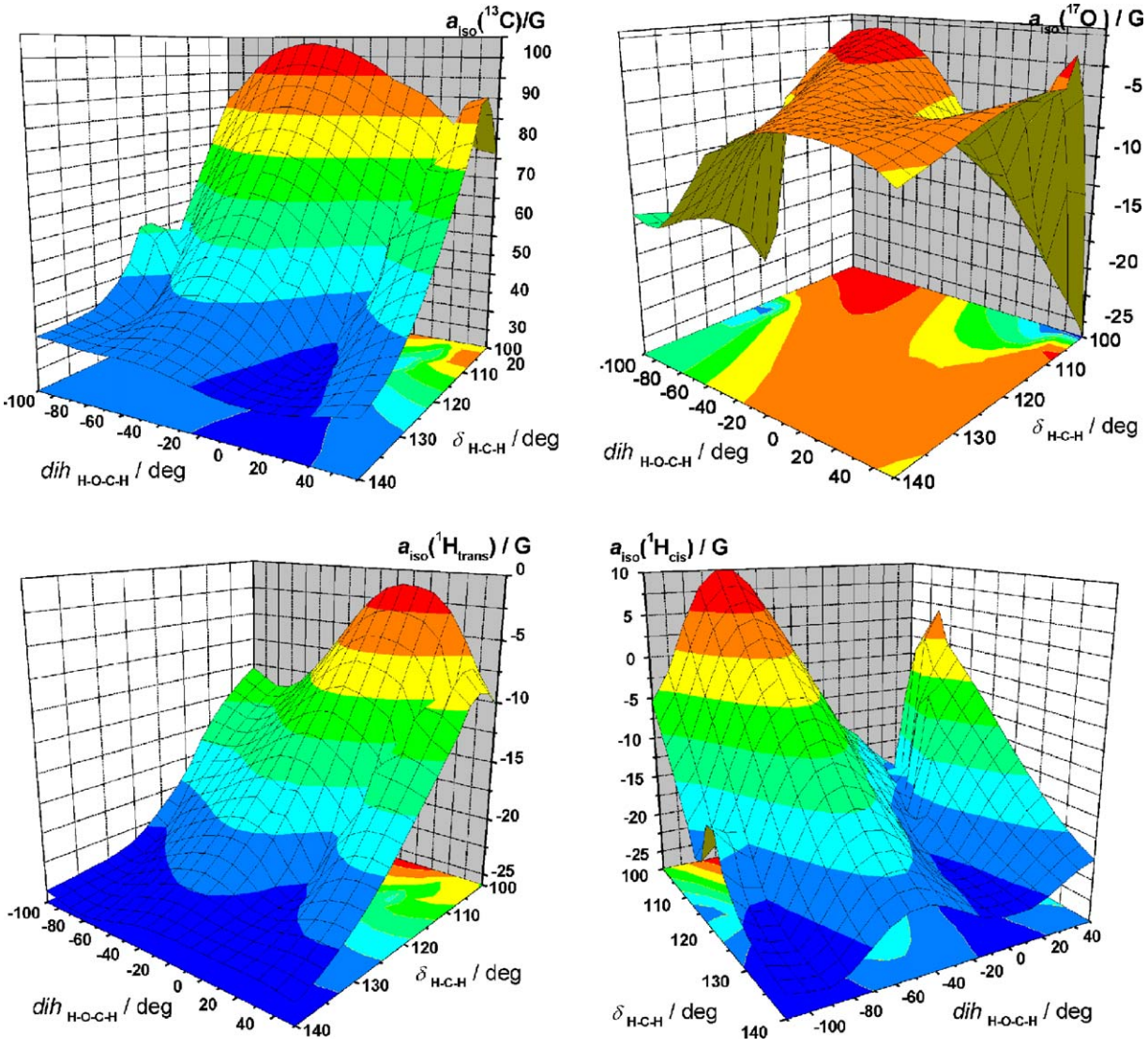

Fig. 3. Variation of the isotropic hyperfine coupling constants of the free hydroxymethyl radical. The $\delta_{H–C–H}$ angle gauges angular deformation of the CH_2 group, whereas the dihedral torsion angle $dih_{H–C–O–H}$ is responsible for twisting of the radical.

angular deformation parameters ($\delta_{H–C–H}$ and $dih_{H–C–O–H}$) are collected in Table 2. As it can be seen, the computed a_{iso} values for carbon and both methylene protons are significantly perturbed by the interactions with the **T5** cluster. In the case of the $a_{iso}(^1H_{cis})$, the observed changes were quite dramatic ranging from −23.75 G for the structure **I** to −5.93 G in the case of the structure **II**, quite similar as in the case of the $a_{iso}(^1H_{trans})$ component. However, despite the fact that for the structure **II** the $\delta_{H–C–H}$ and $dih_{H–C–O–H}$ angles are quite close to those observed in the gas phase radical, both the $a_{iso}(^1H(C))$ values are significantly smaller indicating that the hydrogen bonding renders the H–C bond less prone to polarization. The $a_{iso}(^{13}C)$ value, in turn, was most affected by steric effects when the radical was bound via more distant hydroxyl fragment (structure **I**),

Table 2
The a_{iso} (^{13}C), a_{iso} (^{17}O) and a_{iso} (^1H) for the free $^{\bullet}CH_2OH$ and its van der Waals complexes with the **T5** cluster, along with the values of the associated deformation parameters

Structure	a_{iso} (^{13}C) (G)	a_{iso} (^{17}O) (G)	a_{iso} ($^1H_{cis}$) (G)	a_{iso} ($^1H_{trans}$) (G)	$\delta_{H–C–H}$ (°)	$dih_{H–C–O–H}$ (°)
Free $^{\bullet}CH_2OH$	44.88	−7.52	−15.12	−17.65	120.9	−25.4
I	29.87	−7.78	−23.75	−24.05	124.3	12.5
II	40.63	−7.59	−5.93	−11.07	120.0	−25.9
III	50.48	−10.29	−10.11	−8.54	121.0	10.4
IV	5.60	−8.50	−15.24	−15.47	117.7	−19.6
V	63.50	−1.75	−20.62	−15.16	125.9	−34.4

and not directly through the CH_2 group (structures **II** and **III**). Apparently, a delicate balance between the direct and polarization effects, governing the actual spin density at the carbon nucleus, can be influenced even by such remote interactions quite considerably. The structures **IV** and **V** represent the sites that could be created during dehydroxylation of a surface silanol group, thus, of the strong electrophilic properties. In the case of the structure **IV**, where the radical was bound by a defect center $\equiv Si^+$ via carbon atom, the $a_{iso}(^{13}C)$ was significantly reduced since the involvement of the carbon $2p_z$ in bonding shifted a part of the carbon spin density toward silica.

Finally from the comparison of the calculated and the experimental HFCC (Tables 1 and 2) it can readily be inferred that the hydroxymethyl radical is bound to the silica surface via hydrogen bonding, forming preferentially van der Waals complex of the type **I** structure.

4. Conclusions

EPR $\boldsymbol{g}$ tensor for the Mo_{4c}/SiO_2 and the $\{O^- – Mo_{4c}\}/SiO_2$ surface complexes as well as for the $^{\bullet}CH_2OH$ radicals trapped on the SiO_2 matrix were well reproduced by DFT/GIAO calculations using a spin-restricted ZORA method with the local VWN functional. Isotropic ^{13}C, ^{17}O and ^{1}H hyperfine coupling constants of the surface-trapped hydroxymethyl radical were satisfactory reproduced at the B3LYP/6-311G(df) level. Steric effects resulting from the hydrogen bonds between the silica surface and the $^{\bullet}CH_2OH$ radical give rise to the considerable distortions of the radical to which the $a_{iso}(^{13}C)$ values were the most sensitive. It was found that such distortions of the trapped hydroxymethyl radical have considerable effect on the balance between direct delocalization and spin polarization effects.

Acknowledgements

Financial support by the Committee for Scientific Research of Poland, KBN, grant number 3 T09A 147 26 is acknowledged. The calculations were carried out with the computer facilities of the CYFRONET-AGH, grant number KBN/SGI2800/UJ/018/2002.

References

[1] Z. Sojka, E. Giamello, M.C. Paganini, in: I.T. Horováth (Ed.), Encyclopedia of Catalysis, John Wiley & Sons Inc., Hoboken, New Jersey, 2003, pp. 738–768.
[2] Z. Sojka, M. Che, Appl. Magn. Reson. 20 (2001) 433.
[3] Z. Sojka, M. Che, Colloids Surf. A 158 (1999) 165.
[4] G.H. Lushington, F. Regin, Int. J. Quantum Chem. 106 (1997) 3292.
[5] O. Vahtras, B. Minaev, H. Aren, Chem. Phys. Lett. 281 (1997) 186.
[6] P. Hohenberg, W. Kohn, Phys. Rev. B 136 (1964) 864; W. Kohn, L. Sham, Phys. Rev. A 140 (1965) 1133.
[7] F. Neese, M.L. Munzarova, in: M. Kaupp, M. Bühl, V.G. Malkin (Eds.), Calculation of NMR and EPR Parameters. Theory and Applications, Wiley-VCH, Weinheim, Germany, 2004, p. 21.
[8] E. van Lenthe, P.E.S. Wormer, A. van der Avoird, J. Chem. Phys. 107 (1997) 2488.
[9] G. Schreckenbach, T. Ziegler, J. Phys. Chem. A 101 (1997) 3388.
[10] S. Patchkovskii, G. Schreckenbach, in: M. Kaupp, M. Bühl, V.G. Malkin (Eds.), Calculation of NMR and EPR Parameters. Theory and Applications, Wiley-VCH, Weinheim, Germany, 2004, p. 505.
[11] L.A. Eriksson, O.L. Malkina, V.G. Malkin, D.R. Salahub, J. Chem. Phys. 100 (1994) 5066.
[12] B. Engels, L. Eriksson, S. Lunell, Adv. Quantum Chem. 27 (1996) 297.
[13] M. Munzarová, M. Kaupp, J. Phys. Chem. A 103 (1999) 9966.
[14] P. Pietrzyk, W. Piskorz, Z. Sojka, E. Broclawik, J. Phys. Chem. B 107 (2003) 6105.
[15] L.A. Eriksson, in: M. Springborg (Ed.), Density Functional Methods in Chemistry and Materials Science, Wiley, 1997, p. 125.
[16] E. Pauwels, V. van Speybroeck, M. Waroquier, J. Phys. Chem. A 108 (2004) 11321.
[17] J.A. Weil, J.R. Bolton, J.E. Wertz, Electron Paramagnetic Resonance: Elementary Theory and Practical Applications, Willey & Sons, New York, 1994.
[18] M.-J. Frisch, et al. Gaussian03, Revision B.05, Gaussian Inc., Pittsburgh PA, 2003.
[19] A.D. Becke, J. Chem. Phys. 98 (1993) 5648.
[20] C. Lee, W. Yang, R.G. Parr, Phys. Rev. B 37 (1988) 785.
[21] B. Delley, J. Chem. Phys. 92 (1990) 508.
[22] DMol, InsightII, Release 2000.1, Accelrys Inc., San Diego, CA, 2000.
[23] A.D. Becke, J. Chem. Phys. 88 (1988) 2547.
[24] J.P. Perdew, Y. Wang, Phys. Rev. B 45 (1992) 13244.
[25] J.M. Garrot, C. Lepetit, M. Che, P. Chaquin, J. Phys. Chem. A 105 (2001) 9445.
[26] P. Pietrzyk, J. Phys. Chem. B 109 (2005) 10291.
[27] Z. Sojka, P. Pietrzyk, Spectrochim. Acta A 60 (2004) 1257.
[28] G. te Velde, F.M. Bickelhaupt, S.J.A. van Gisbergen, C. Fonseca Guerra, E.J. Baerends, J.G. Snijders, T. Ziegler, J. Comput. Chem. 22 (2001) 931.
[29] ADF2002.03, SCM, Theoretical Chemistry, Vrije Universiteit, Amsterdam, The Netherlands, http://www.scm.com.
[30] E. van Lenthe, E.J. Baerends, J.G. Snijders, J. Chem. Phys. 99 (1993) 4597.
[31] S.H. Vosko, L. Wilk, M. Nusair, Can. J. Phys. 58 (1980) 1200.
[32] Z. Sojka, M. Che, J. Phys. Chem. 99 (1995) 5418.
[33] Z. Sojka, M. Che, J. Phys. Chem. 100 (1996) 14776.
[34] Z. Sojka, M. Che, Bull. Pol. Acad. Sci. 48 (2000) 313.
[35] S. Patchkovskii, T. Ziegler, J. Chem. Phys. 111 (1999) 5730.
[36] P.J. Krusic, P. Meakin, J.P. Jesson, J. Phys. Chem. 75 (1971) 3438.
[37] R. Livingston, H. Zeldes, J. Chem. Phys. 44 (1966) 1245.
[38] V. Barone, in: D.P. Chong (Ed.), Recent Advances in Density Functional Methods, Part I, Word Scientific Publ. Co., Singapore, 1996.